IEEE Access
Multidisciplinary | Rapid Review | Open Access Journal

Received July 8, 2019, accepted August 5, 2019, date of publication August 9, 2019, date of current version August 22, 2019.

Digital Object Identifier 10.1109/ACCESS.2019.2934175

An Overview of DC Component Generation, Detection and Suppression for Grid-Connected Converter Systems

BO LONG[1], (Senior Member, IEEE), MUHENG ZHANG[2], YONG LIAO[1], LIJUN HUANG[3], AND KIL TO CHONG[4], (Member, IEEE)

[1]School of Mechanical and Electrical Engineering, University of Electronic Science and Technology of China, Chengdu 611731, China
[2]Department of Electrical Engineering and Computer Science, University of California at Irvine (UCI), Irvine, CA 92697, USA
[3]Guangzhou Haige Communication Group Incorporated Company, Guangzhou 510663, China
[4]Department of Electronic Engineering, Chonbuk National University, Jeonju 54896, South Korea

Corresponding author: Kil To Chong (kitchong@jbnu.ac.kr)

This work was supported in part by the Fundamental Research Funds for the Central Universities of China under Grant ZYGX2016J115, in part by the Brain Research Program of the National Research Foundation (NRF) funded by the Korean Government (MSIT) under Grant NRF-2017M3C7A1044815, in part by the State Key Laboratory of Control and Simulation of Power System Generation Equipment, China, under Grant SKLD17KM09, in part by the Tsinghua University, China, in part by the Visiting Scholarship of the State Key Laboratory of Power Transmission Equipment and System Security and New Technology, Chongqing University, China, under Grant 2007DA10512716415, and in part by the National Natural Science Foundation of China under Grant 51607027.

ABSTRACT Transformerless grid-connected distributed photovoltaic (PV) systems (TGCDPVs) has the merits of high efficiency, small size, and low cost, draws great interest in recent years. However, Direct Current (DC) injection is a serious issue in TGCDPVS, which degrade its power quality. Some publications have discussed DC component generation and suppression methods; however, there are very few systematic reviews on the generation, detection, and suppression of DC component in TGCDPVS. For young researchers and designers working in photovoltaic power generation systems, the DC injection suppression is of great importance. This paper first reviews a number of issues related with dc component in TGCDPVs, the DC current generation and its detriments to the grid are reviewed at first, then, a comprehensive review on the latest DC detection method are performed, finally, various DC suppression solutions are given. Comparisons between various DC component detection and suppression methods are discussed. In the end, some future suggestions are given. This review shall provide a useful guideline and a clearer vision for researchers to determine the best solution for DC suppression in their PV product.

INDEX TERMS Photovoltaic system, grid-connected converter, DC component detection, power quality.

NOMENCLATURE

ABBREVIATIONS

DC	Direct current.
PCC	Point of common coupling.
PR	Proportional resonance.
QPR	Quasi proportional resonance.
PID	Proportion-integration-differentiation.
PLL	Phase-locked loop.
THD	Total harmonic distortion.
MPPT	Maximum power point tracking.
GCCs	Grid connected converter system.
SWDIM	Sliding window double integration method.
DG	Distributed generation.
PV	Photovoltaic.
VC	Virtual capacitor.
PF	Power factor.
DSP	Digital signal processor.
FPGA	Field Programmable Gate Array.
TGCDPVS	Transformerless grid-connected distributed photovoltaic systems

The associate editor coordinating the review of this article and approving it for publication was Junjian Qi.

I. INTRODUCTION

With the gradual exhaustion of fossil energy in the world, energy shortage becomes a significant problem for countries in the world. Since the solar and wind energy resource are widely distributed, abundant and non-polluting,

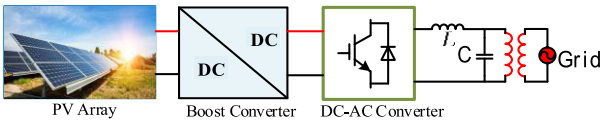

FIGURE 1. Grid-connected converter system with the line-frequency transformer.

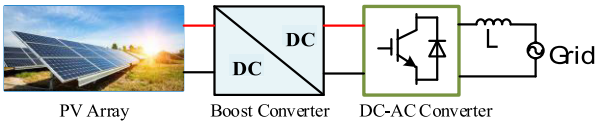

FIGURE 2. Grid-connected converter system without transformers.

many attempts have been presented on the usage of these resources [6], [7]. Grid connected converter plays an important role in the high-quality energy conversion in distributed generation system DGs.

There are two schemes for grid-connected converter in the distributed power generation system, namely, isolation and non-isolation power converters. For isolation schemes, Fig. 1 demonstrates a diagram of GCDPVS that employs a line-frequency transformer, which can achieve voltage matching and electrical isolation [10]. The isolation transformer means that no direct current (DC) is injected to the grid. The advantages of this scheme are: firstly, the simplified power circuit and control circuit; secondly, much lower DC-link voltage is required than that in transformerless grid-connected converter for voltage matching at PCC. However, the line-frequency transformer has drawbacks of high system cost, low overall system efficiency, over-weight, and large volume [11], [12]. To solve the above issues, the TGCDPVS draws great interests in recent years.

A general topology of non-isolated GCCs is shown in Fig. 2, which shows many advantages and are widely used in small-power and low voltage applications. Calais shows that the cost of converters without transformer is less than those with transformers by 25% [15]. Also as discussed in [12] and [18], the system efficiency using transformerless scheme increases by about 2%.

The transformerless grid-connected scheme is adopted to many power generation system due to much lower power, smaller size, and higher efficiency [19]. However, this scheme introduces the DC injection issue, which has enormous impacts on the power quality of the grid, mentioned in Section II-B. Many countries and organizations (e.g., IEEE Standard 1547-2003) have setup maximum allowable DC current injection standards to limit the level of the DC component. It is necessary to investigate the DC component issues in TGCDPVs.

To the author's knowledge, until now, few review literatures have been found on discussing dc component generation, detriments, detection and suppression. As a result, this paper aims to present a comprehensive review on the aspects of DC component issues in GCIs for engineers and researchers working in renewable energy generation control. Generation and detriments of dc component on the influences for the power quality in the GCCs are discussed at first, then latest dc component detection, and suppression methods (e.g., power converter with DC suppression capability, physical capacitors, virtual capacitors, intelligent compensation control, etc.) are also reviewed.

This paper is organized as follows: Section II reviews the generation and detriments of DC component in TGCDPVs. Section III reviews the DC detection methods in terms of feasibility, economy, reliability, and efficiency. Section IV summarizes all the latest techniques on DC suppression, and comparisons results between these methods are presented. Finally, section V concludes this paper and gives potential research works on this area.

II. GENERATION AND DETRIMENTS OF DC COMPONENTS IN TRANSFORMERLESS GCIS

In this section, we will first analyze the generation of DC component in GCIs, then, the detriments of DC component on the instruments and loads in the micro-grid system will be discussed.

A. GENERATION OF DC COMPONENTS

In this section, we will first analyze the generation of DC component in GCIs, then, the detriments of DC component on the grid connected system will be discussed. According to the literatures in [20], [21], and [22], the introduction of DC injection is mainly caused by five reasons, which can be discussed as followings.

1) ASYMMETRICAL GATE DRIVING SIGNALS AND DISPARITY OF POWER TRANSISTORS

The inconsistent operation of power devices introduces DC components in the output current. The source can be divided into two aspects: (1). The driving circuit for each power transistor may not be uniform, for example, time-delay on the device turn-on/off voltage, and turn-on/off driving current may also varies between power transistors. As a result, the PWM (Pulse-Width-Modulation) signals are also asymmetrical. (2). The switching devices are not always identical (e.g., saturation voltage, leakage current, distributed parameters, junction capacitance, etc.). As a result, disparities of the power transistors may also generate DC components in the grid current [20]. The two sources result in the inconsistent operation of power devices, introducing the DC component in the grid current.

2) DC COMPONENTS IN THE REFERENCE CURRENT

The power quality of the grid current reference is another factor that may introduce DC component. The controller strategy for grid-connected converter usually adopts double closed-loop control structure including outer voltage loop and inner current loop. The voltage loop output is serving as the input current reference of the current controller in the inner loop. The frequency of the control loop is generally equivalent to the switching frequency. However, as shown

in Fig.4, the amplitude of output current reference may not be entirely symmetrical due to the influences of voltage feedback and control performance. Therefore, the grid current reference may contain DC components, so as the DC component in the grid current. Consequently, it is needed to ensure the reference grid current in the closed-loop does not contain any DC components.

3) ZERO-DRIFTS AND SCALING ERRORS OF CURRENT AND VOLTAGE SENSORS IN THE SAMPLING CIRCUIT

In the nonlinearity of ac voltage and current sensors, and operational amplifiers, the zero-drift and scaling error may lead to the generation of DC components. In the closed-loop control scheme for grid-connected inverters as shown in Fig.4, it is usually needed to measure the grid current and voltage, filter capacitor current and voltage, and feedback them to the microprocessor [21]. During this procedure, the sampling biases due to zero-drift, scaling error, as well as nonlinearity of Hall sensor and operational amplifier cannot be ignored and may lead to DC components injection [22]. In utility, even small measurement deviations may be amplified by forward-loop controller and introducing non-negligible DC component in the grid current.

4) DC VOLTAGE IN GRID VOLTAGE

In three-phase GCCs, the unbalanced phase-voltage and existing DC component in the grid voltage may also generate DC component.

Fig. 3 shows the relationship between grid current $i_g(s)$ and converter voltage $\upsilon_{inv}(s)$ and grid voltage $u_g(s)$.

For an LCL-type voltage-source GCIs, $i_g(s)$ can be described as (1).

$$i_g(s) = \frac{1}{L_{inv}L_gC_fs^3 + (L_{inv}+L_g)s} \cdot v_{inv}(s) + \frac{L_{inv}C_fs^2+1}{L_{inv}L_gC_fs^3 + (L_{inv}+L_g)s} \cdot u_g(s) \quad (1)$$

where L_{inv} is the converter-side inductance, L_g is the grid-side inductance, C_f is LCL filter capacitance, υ_{inv} is converter-side voltage and u_g is grid voltage. From (1), the DC components can be generated by two sources: converter-side voltage $\upsilon_{inv}(s)$ and grid-voltage $u_g(s)$. Also, according to (1), due to the none-zeros in numerator, the system itself cannot suppress the DC components generated by converter-side and grid-side voltage. For the converter-side voltage, it can be influenced by the switching behaviour of the power switches and the power converter topology. The unbalanced voltage and DC voltage in the grid may also have impacts on DC injection. In an ideal grid voltage, no DC component should exist. However, the grid current may contain DC component if the loads are asymmetrical. This may finally magnify the DC injection.

5) SAMPLING ERRORS IN ADC CONVERSION

Nowadays, high-speed microprocessor (such as DSP and FPGA, etc.) has been widely used in the digital control of the GCI system, all the output information of ac current and voltage sensor has been digitalized and sent to the ADC port of the microprocessor. However, due to some unavoidable voltage-bias in the sampling circuit, the biased ADC results of the analog signals may have sampling errors, which may also generate DC component in the grid current.

To summarize the above contents, Fig. 4 shows all the possible sources that may generate DC components in GCCs.

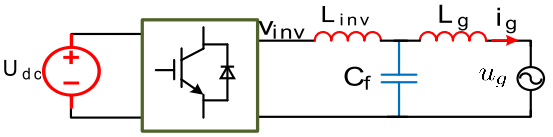

FIGURE 3. Topology of an LCL-type grid-connected voltage source converter.

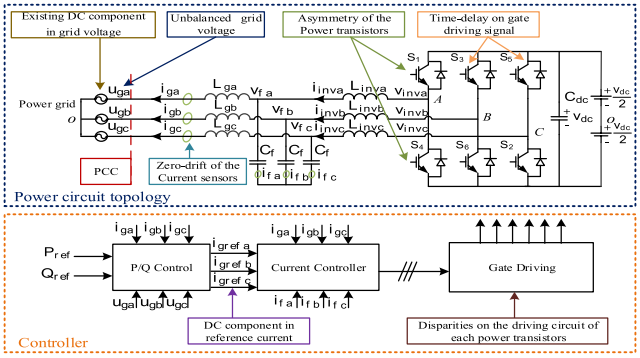

FIGURE 4. Generation of DC components in an LCL-type TGCPVS [23].

TABLE 1. Detriments of DC injection [8]–[14].

Index	Detriments of DC components
1	Magnetic current, transformer saturation, reduced service life time of transformer.
2	Accelerates corrosion in grounding cables and metal, increased network cabling.
3	Pulsating torque, eddy current, noise, and overheating of AC electrical machine.

B. DETRIMENTS OF DC INJECTION

In [24], Salas proved the existence of direct current injection into the grid from converters, using twelve single-phase converters (according to the transformer options: 50 Hz LF (Low-Frequency) transformers, HF (High-Frequency) transformers or transformer-less) from the European market. The conclusion is that the DC injection exists in all cases. According to the research results presented by Armstrong *et al.* [13], Blewitt *et al.* [19], and Enders *et al.* [25], the detriments of DC injection to the grid can be summarized and illustrated in Table 1.

To prevent the negative impacts of DC injection, many countries have enacted regulations to limit the DC injection from the PV systems. In [26], the author summarized the legislations in some countries and Table 2 shows the standards on DC injection in these countries and IEEE organizations.

TABLE 2. Regulations on DC current injection limitations [26]–[28].

Country	Maximum DC current
AUSTRALIA	5 mA
CHINA	0.5% rated output current
GERMANY	1000 mA
JAPAN	1% rated output current
UK	5 mA
USA	0.5% rated output current
IEEE 929-2000	0.5% rated output current

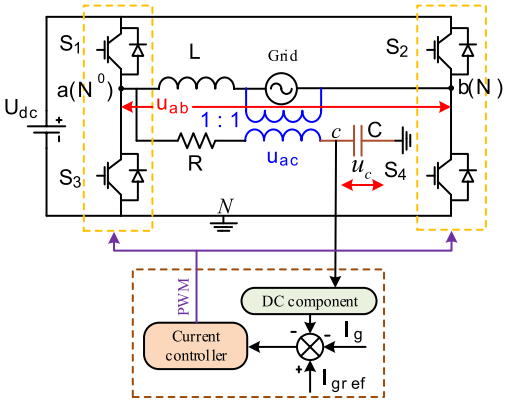

FIGURE 5. Parallel transformer method for DC component detection.

III. DC COMPONENT DETECTION METHODS

Compared to the RMS value of ac component, the DC component in the grid current is very small, whether the DC component can be accurately measured determines the suppression effect. According to recent literatures, the current research on DC detection can be categorized by hardware and software methods.

A. DC COMPONENT DETECTION USING ADDITIONAL CIRCUITS

1) WITH ADDITIONAL TRANSFORMER

As shown in Fig. 5, Sharma proposed a method using the parallel transformer to determine the DC component [1], and Ahfock and Bowtell [2] studied its mathematical model, including DC offset sensor and feedback system. In Fig.5,I_g, I_{gref}, and U_g represent grid current, reference grid current, and grid voltage, respectively. Another circuit is parallel with the output of the converters, and the turn ratio of the transformer is perfectly 1:1. Assuming that the AC component and DC component in the voltage across point a and b is u_{ab} and u_{dc}, respectively, which can be described in (2) and (3).

$$u_{ab} = u_{ac} + u_{dc} \tag{2}$$

$$u_{aN} = u_R + u_{ac} + u_c \tag{3}$$

When S_1 and S_4 switch on, $u_{ab} = u_{aN}$, from (2) and (3), the DC component can be written in (4).

$$u_{dc} = u_R + u_c \tag{4}$$

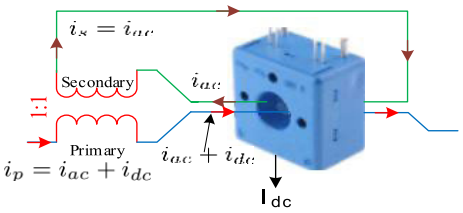

FIGURE 6. Parallel connected transformer with hall sensors in the opposite current direction for DC detection [3].

From (4), the voltage-drop across the capacitor C is the DC component existed in the grid when the system enters steady state. By using the proposed current controller, the reference current can be adjusted to suppress the DC component.

However, this method is impractical in utility. From [2], the AC component is 0 when the leakage flux of the transformer equals 0. That is, it needs a large core and small resistance of windings. However, in practice, the leakage flux cannot be 0, and the requirements for small leakage flux will increase the cost of this scheme dramatically.

Based on the similar idea, Abdelhakim proposed a more practical method [3]. As shown in Fig. 6, the current of both winding flows through the Hall sensor in the opposite direction, which results in the magnet field cancellation generated by the primary and secondary current. As a result, only the DC component left, and is measured. Hence, the small range Hall sensor can be used to measure the DC component.

To be more specifically, i_p and i_s represent the current that flows through the primary-side and the secondary-side, respectively. i_{dc} and i_{ac} represent the ac and dc component in the grid current, respectively, which can derived by (5).

$$I_{dc} = i_p - i_{ac} = i_{ac} + i_{dc} - i_{ac} = i_{dc} \tag{5}$$

From (5), output of the current sensor I_{dc} in the circuit will only contain DC components because of the magnetic field cancellation principle.

In essence, this scheme utilizes the operation principles of magnetic field cancellation to get DC component. To achieve much higher accuracy, it is of great importance to consider some factors.

- It is needed to minimize the leakage inductance and secondary winding resistance to reduce the magnetizing current and power losses.
- To get better DC extraction performance, the material for the transformer's magnetic core with higher permeability is better, which can decrease its turns and increase the magnetizing inductance.
- To acquire high-resolution DC component extraction, the parallel-connected transformer cannot be saturated in this procedure.

2) WITH TWO-STAGE SINGLE-ORDER CIRCUIT

Bowtell and Ahfock [4] proposed an improved method based on the detection and compensation method. Fig. 7 shows the detection module, which is composed by the additional

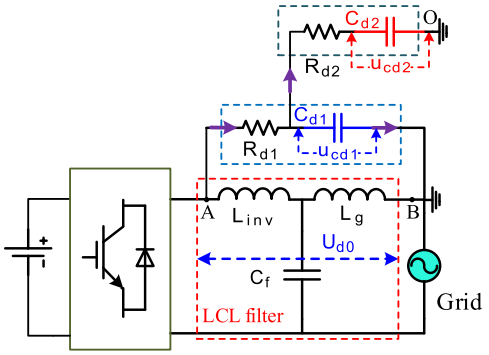

FIGURE 7. Two-stage single-order DC component detection circuit for an LCL-type grid connected converter.

circuit, where U_{d0} is the voltage-drop between A and B, u_{cd2} is the voltage-drop across the capacitor C_{d2}, u_{cd1} and u_{cd2} are the voltage-drop on C_{d1} and C_{d2}, which are used to block the DC component of the converter-side voltage. u_{cd2} would be the DC component extracted from the converter-side voltage.

From Fig. 7, the voltage ratio between u_{cd2} and u_{cd1} is given by (6) as

$$\frac{u_{cd2}}{u_{d0}} = \frac{1}{\tau_d^2 s^2 + 3\tau_d s + 1} \tag{6}$$

where $\tau_d = R_{d2} \cdot C_{d2}$, $U_{d2}(0) = 0$, R_{d2} and C_{d2} is the resistance and capacitance of the filter, and the derivate of $U_{d2}(0)$ also is equal to 0. From (6), the ratio between u_{cd2} and u_{cd1} at 0 Hz is 1, which indicates that the DC component in u_{d0} can be indirectly obtained by measuring the voltage drop across the capacitor C_{cd2}.

In a word, the two-stage single-order circuit has the advantage of having almost no influences on other control systems, such as DC bus voltage control and MPPT control. It has better independence and is an ideal circuit topology for DC component sampling. However, it is essential to choose the proper value of resistance and capacitance. Specifically, if their value is too small, it will lead to the injection of high-order harmonics to the grid. If their value is too large, it cannot measure the required DC voltage accurately. If the resistance R_{d2} is increased to acquire high dc component detection accuracy, its power losses will also be increased. What is more, another disadvantage is that this scheme requires one more two-stage single-order circuit to determine the voltage, which makes the system more complicated. However, this scheme has the advantages of almost no influences on the original control system, such as DC bus voltage control and MPPT control.

3) PARALLEL CONNECTED RESONANCE CIRCUIT

Another solution for DC component detection is using an auxiliary resonant circuit, Ahmed and Li proposed a precise detection method to determine the DC injection from single-phase converters [5]. Fig. 8 shows the proposed DC component measurement circuit, where L_{res} and C_{res} operates together to form a resonant circuit. υ_m is the voltage-drop on the sampling resistance R_m.

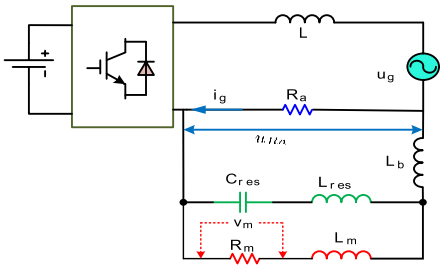

FIGURE 8. DC component detection using a resonant circuit [5].

From Fig. 8, the transfer function from grid current $i_g(s)$ to output voltage $\upsilon_m(s)$ can be expressed as (7).

$$G_m(s) = \frac{v_m(s)}{i_g(s)} = \frac{R_m R_a}{(R_a + sL_b)\dfrac{\left[R_m + s(L_m + L_{res}) + \frac{1}{sC_{res}}\right]}{\left(sL_{res} + \frac{1}{sC_{res}}\right)} + (R_m + sL_m)} \tag{7}$$

This circuit is based on the resonance method to determine the DC component. The resistor R_a is a resistive current shunt in the path of the inverter output current. The filter resonance inductance L_{res} and capacitance C_{res} are connected in series to bypass the majority of the fundamental ac component across the shunt and block the DC component. As a result, the entire dc component of the shunt resistor voltage will be applied across the resistor R_m as C_{res} is blocking the dc component. L_b is used to block the main inverter current ac component while L_m is used to force the ac signal to circulate through L_{res}-C_{res} branch. L_b and L_m are very important to block most of the ac signal increasing dc component ratio in the output signal. υ_m is measured as an indication of the dc component contained in the inverter output current, which contains a residual of the 50 Hz (or 60 Hz) ac component that has not been filtered out in spite of the last discussion. Nevertheless, this method has little effect as long as much of the ac component has been bypassed and the signal-noise ratio regarding the targeted dc component in the measured current shunt voltage is significantly improved. It is needed to note that the parameters of the resonant circuit should be in high accuracy to bypass the ac component of the grid, which increases the cost of the system.

4) DETECTION METHODS BASED ON REACTORS

Buticchi, Lorenzani, and Franceschini proposed a compensation method using a few cheap passive components and a simple algorithm [8], [9]. In this method, if a DC voltage is superposed to a sinusoidal voltage waveform, the reactor's magnetic flux will saturate asymmetrically, and its current will be distorted at a voltage zero-crossing, which is a basic theory of this method.

Firstly, the saturation magnetic circuit is used to measure the DC component in the output current of the converter. The

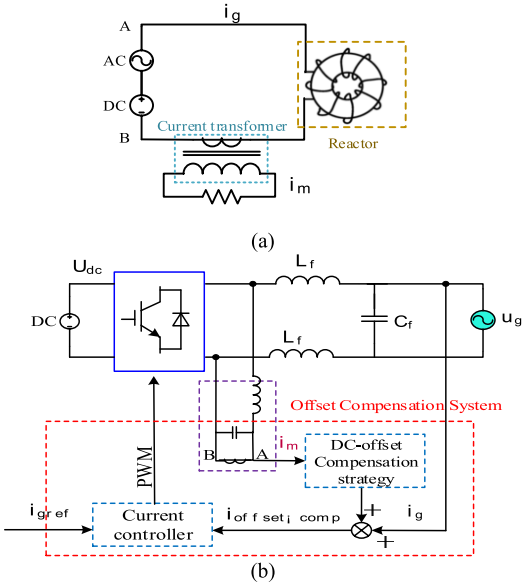

FIGURE 9. Block diagram of the DC offset compensation system based on saturable magnetic circuit. (a) Diagram of the saturable magnetic circuit. (b) Block diagram of the DC-offset compensation system.

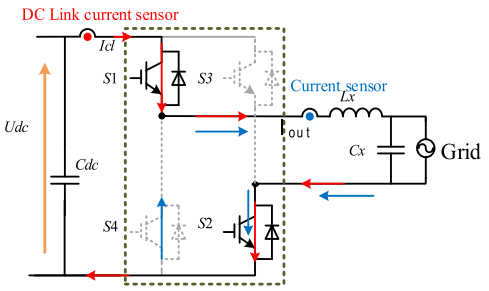

FIGURE 10. The topology of the auto-calibrating DC link current sensing technique in a half bridge converter.

exemplification diagram of this saturation magnetic circuit is shown in Fig. 9, where the voltage-source models the sinusoidal and DC component. The reactor current is measured by a current transformer whose output is i_m.

In this scheme, the detection branch is simple, and it is able to eliminate errors caused by sensors. However, it is hard to make the reactor exactly magnetic saturation. Besides, the results are easily to be influenced by the environment.

5) DC COMPONENT AUTO-CALIBRATING METHOD

According to the literature proposed by Armstrong *et al.* [13], a DC auto-calibration method is proposed, as shown in Fig. 10, the power circuit configuration is the H-bridge converter, which contains two current sensors in the system for DC-link and grid current detection.

In Fig. 10, the auto-calibrating DC-link current sensing technique with unipolar switching scheme has four switching states shown in Table 3. Taking state 1 and 3 as an example, When S_1 and S_4 switches ON (state 1), the DC-link current I_{cl} is equal to the grid current i_g. when S_1 and S_3 switches OFF (state 4), the inductor current flows through the by-pass

TABLE 3. Switching states of an unipolar switched H-bridge Converter.

State	S_1	S_4	S_3	S_2	DC Link Current
	Leg 1		Leg 2		
1	ON	OFF	OFF	ON	I_{cl}
2	OFF	ON	ON	OFF	I_{cl}
3	ON	OFF	ON	OFF	0
4	OFF	ON	OFF	ON	0

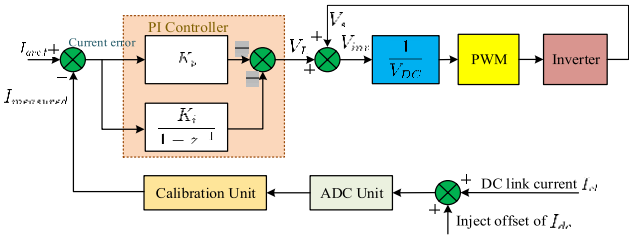

FIGURE 11. Implementation of the auto-calibrating DC-link current sensing.

freewheeling diode of S_2 and S_4, during this interval, the DC-link current I_{fl} should be 0 in an ideal condition.

Table 3 gives all the possible switching states of the proposed scheme, The DC-Link current I_{out} various according to the corresponding switching states of the power transistors, During the conduction stage (stage 1 and 2), the output current can be measured by the hall current sensor. During the freewheeling stage (stage 3 and 4), the detected current from the DC-link current sensor should be 0 theoretically. In fact, due to some reasons, the measured current does not equal to 0 due to the errors caused by current sensor. Calibration for sensor measurement I_c, which is applied to PI controller, is obtained by subtracting freewheel loop current I_{fl} from conducting loop current measurement I_{cl}. The realization of this scheme is illustrated as Fig. 11.

The experimental results in [13] show the method can limit the DC component to 8.63 mA in a 50 Hz, 10 A RMS converter output current with 70-mA preset DC-offset.

This scheme is easy to implement without additional circuits. But it is only suitable for eliminating the DC component caused by the zero-drift of Hall sensors. It cannot mitigate the DC injection caused by other factors. Based on the same idea, Berba, Atkinson, and Armstrong applied this idea on a three-level half-bridge converter [14], where the auto-calibrating DC-link current sensing in a three-level half-bridge power converter was utilized.

6) SLIDING WINDOW DOUBLE INTEGRATION METHOD

Beside hardware dc detection method, In [16], the author proposed a real-time DC injection detection method using software. Theoretically, the grid current can be composed by fundamental frequency component, harmonic frequency component, and dc component. To be more specific, the grid current can be expressed as

$$I_g(t) = I_{dc} + I_{ac} = I_{dc} + \sum_{n=1,2,3,\ldots} I_n \sin(2\pi n f_1 t + \varphi_n) \quad (8)$$

TABLE 4. Comparisons between different DC component detection methods.

DC detection methods	Advantages	Disadvantages
Methods based on additional transformers [1-3].	• Simple in design. • No influences on the original system, more independently.	• Hard to make transformer with exact turn ratio 1:1. • Extra power loss. • Additional cost. • Large volume due to the line-frequency transformer.
Two-stage single-order circuit [4].	• Almost no influences on the original control systems. • The cost for additional DC component sampling is very cheap.	• Additional detection circuit. • Parameters of the RC circuit are hard to choose. • The accuracy of DC component detection results is easily influenced by the component parameters.
Parallel connected resonance circuit [5].	• High accuracy even in small DC component measurement.	• Additional detection circuit. • Additional cost to the system. • High resolution passive components are needed.
Methods based on reactor [8, 9]	• The detection branch is simple. • Eliminate errors caused by sensors when the sensors directly sampling. • Fully isolated from the original circuit.	• Hard to make the reactor exactly magnetic saturable. • Easily influenced by environment. • Existing small errors for the 2nd harmonic. • The DC bias is nonlinear.
Auto-calibrating method [13, 14]	• Simple in design. • No additional auxiliary circuit. • No need for complex control algorithm.	• Accuracy will decrease when the duty cycle is small. • Unsuitable for bipolar PWM modulation. • Only solving the DC injection caused by hall sensor.
Sliding window double integration method [16, 17]	• High accuracy. • High robustness. • Compensating harmonics. • Small influences by noise. • No additional circuit, no extra expense.	• Hard to balance between the integration number and the dynamic response. • Additional time-delay.

where I_{dc} and I_{ac} are the dc and ac component in the grid current, respectively. Besides, in (8), I_{n}, nf_1 and φ_{n} are the amplitude, frequency, and phase-angle of ac components, respectively. When after integrating (8), the I_{ac} is close to 0 under the condition that the integration period T is the same with the grid period T_{grid}.

To achieve much higher dc detection resolution, two times integration of $I_{\mathrm{dc}}(\mathrm{t})$ are performed, which is shown in (9).

$$\begin{aligned} & I_{dc1}(t) \\ & = \frac{1}{T^2}\int_{t_0}^{t_0+T}\int_{t_0}^{t_0+T} I_g(t)dt \\ & = \frac{1}{T^2}\int_{t_0}^{t_0+T}\left[\int_{t_0}^{t_0+T}(I_{dc}+\sum_{n=1,2,..} I_n\sin(2\pi nf_1t+\varphi_n))dt\right]dt \\ & = I_{dc}+\sum_{n=1,2,.}\left[\frac{f_{grid}}{\pi nf_1}\sin\left(\frac{\pi nf_1}{f_{grid}}\right)\right]^2 \\ & \quad \times I_n\sin\left(2\pi nf_1t+\varphi_n+\frac{\pi nf_1}{f_{grid}}\right) \\ & \approx I_{dc} \end{aligned} \tag{9}$$

From (9), when the differences between f_1 and f_{grid} is pretty small, Hence, the DC estimation error can be minimized by multiple times of integrations. Based on this idea, In [17], Jiang and Yuan proposed a method called Moving Average Filter (MAF) to detect the dc component based on the multiple integration method. The moving average filter is represented as (10). x and y are the input and output of the filter in time domain, respectively, the sampling points $N = 100$.

$$y[n] = \frac{1}{N}\sum_{k=0}^{N-1} x[N-k] \tag{10}$$

As shown in Fig.12, in one sampling window, the current sensor sampling points N=100, the newest sample results will override the oldest sampling results in the sampling window and will calculate the updated average value periodically.

This method uses moving average algorithm to replace the traditional low-pass filter. The ac component is eliminated when it passes through the filter. Compared to low-pass filter, this method has much higher accuracy in filtering and faster dynamic response. It also has better performance in harmonics compensation because it has 0 gain at n×50 Hz (n=1, 2, 3· · ·).

Summarizing the above dc detection methods, comparisons between different DC detection methods are shown in Table 4.

IV. DC COMPONENT SUPPRESSION METHODS

Based on the literature review on DC component introduction and detection, dc component suppression methods will be introduced.

A. DC CURRENT SUPPRESSION CONVERTER

The literatures in González *et al.* [20], [29], Wu *et al.* [30], and Shimizu *et al.* [31] show that the half-bridge converters can mitigate the DC current injection, which is a commonly used method to limit the DC component. As shown in Fig. 13,

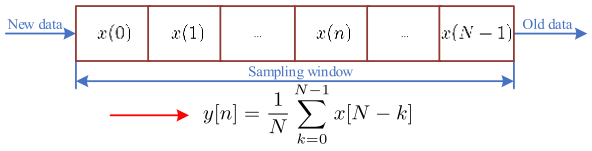

FIGURE 12. Sampling window of the moving average filter.

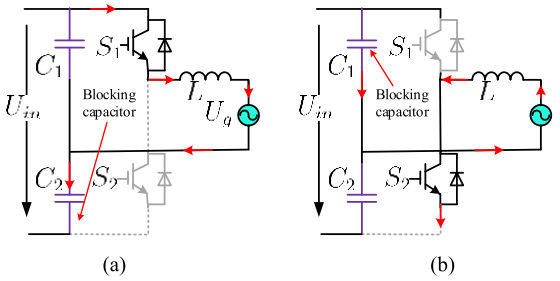

FIGURE 13. Half-bridge converter with DC component suppression capability. (a) The output current when S1 turned on. (b). The output current when S2 turned on.

the current always flows through the capacitor in all situations and the DC component is eliminated by the capacitors (C_1 and C_2).

The drawbacks of the scheme in Fig. 13 are that half-bridge power converter is usually suitable for small power systems, which limits its application in medium or large power areas.

Compared with full-bridge topology, half-bridge converters have the half of the voltage output as full-bridge converter, and their DC input is twice as much as full-bridge converters. In this way, the voltage stress of switching devices in half-bridge topology is enormous, which results in relatively slow switching action and high switching loss. Furthermore, the blocking capacitors C1 and C2 may not be uniform during the switching period. Active and passive based voltage balanced control methods are usually necessary in Fig. 13.

To extend this idea into higher voltage applications, Gonzalez Gubia and Lopez proposed a single-phase half-bridge multilevel converter, which can suppress the DC injecting into the grid [20]. From [20], [30], compared with two-level half-bridge converters, the single-phase three-level diode clamped converter has many advantages, such as the higher efficiency, lower current ripple, and total harmonic distortion.

B. DC CURRENT COMPENSATION METHODS

Another DC current suppression method is realized by utilizing compensation control. The basic theory of the DC component detection and compensation method is illustrated in Fig. 14, where U_{dc}, U_g, and i_g represent the DC voltage, grid voltage, and grid current, respectively. U_{dcref} and i_{dcref} represent the DC-link input voltage reference and grid current reference, respectively. Besides, i_{gdc} is the DC component existing in the grid current and the i_{dccomp} is the compensation current generated by the compensation control block.

The operation principle of the DC component detection and compensation method are described as: first, the DC component of grid current is measured, and the compensation

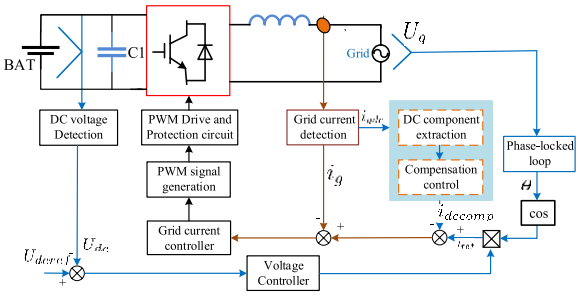

FIGURE 14. Block diagram of the DC component detection and compensation method.

is generated by the appropriate control algorithm, then the output of compensation control block i_{dccomp} is fed back to the reference signal or modulation signal of grid-connected current. Finally, the switch will be controlled by the regulator, and the DC component is suppressed.

The effectiveness of this method relies much on the accuracy of DC component extraction result and current sensor sampling result; consequently, the DC component generated by the disparities of power transistors in the power circuit can be successfully mitigated, however, it cannot realize DC component suppression generated by the zero-drift and scaling error of current sensors.

To reduce the errors that may be generated by current sensors, He, Xu and Chen proposed a control strategy to suppress the DC injection based on measuring the line-line voltage output of the converter (U_{AB}) precisely [32], which is a voltage filtering DC extraction approach. As shown in Fig. 15, an additional DC suppression loop is added to the system to minimize the DC component. More specifically, a differential amplifier and low-pass filter are used to extract the DC offset voltage from the inverter voltage which is compared with the reference DC-offset voltage and manipulated by a PI controller. The output of DC suppression loop controller is synthesized to the grid current reference to control the power circuit.

This method indirectly eliminates the DC component in the grid current by way of suppressing the DC component at the output voltage of the converter, which does not need the DC current sensor, as a result, compared with the method in [32], the performance of DC component suppression is greatly enhanced.

In addition to the DC mitigation method using voltage feedback, as shown in Fig. 16, a PI controller, which uses the DC component in grid current, is used in the DC suppression loop [32].

From Fig. 16, the transfer function from the disturbance source $U_{dis}(s)$ to grid current $I_g(s)$ is obtained in (11).

$$\frac{I_g(s)}{U_{dis}(s)} = \frac{s \cdot e^{-(sT_s)}}{s(sL + r) + K_1 K_G (K_{pi} s + K_{ii})} \tag{11}$$

From (11), the DC current suppression effect is much better than those without suppression loop are. However, this

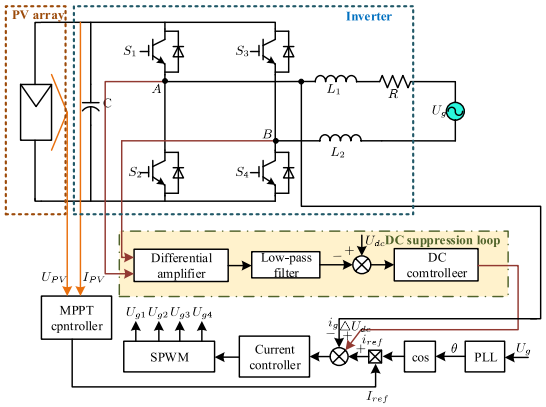

FIGURE 15. DC component suppression scheme of a PV grid-connected converter with line-line voltage output control.

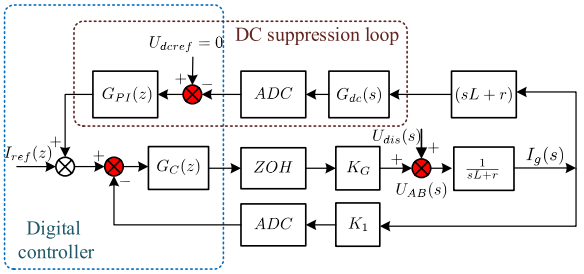

FIGURE 16. Control diagram with DC suppression control loop.

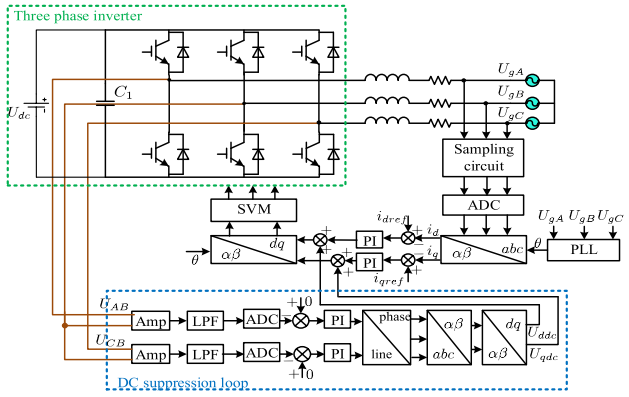

FIGURE 17. Block diagram of a three-phase PV grid-connected converter with DC component suppression control.

additional loop increases the complexity of the control scheme and requires high-speed microprocessors.

Besides the scheme in [30], similar ideas are also used in three-phase GCC to suppress the DC component. In [33], as shown in Fig. 17, similar to the method above, two additional DC suppression loops are added. The differential amplifier and low-pass filter can filter the fundamental and high frequency components to extract the DC components in the converter-side voltage. The outputs of the PI controller are line voltages, which should be transformed into dq-frame by utilizing the Clark and Park transformation matrixes,

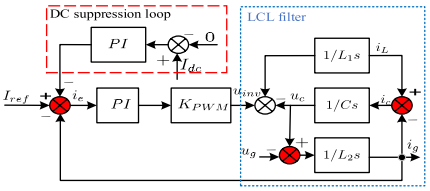

FIGURE 18. Block diagram of the dc component mitigation control method in [34].

$T_{line/phase}$, $T_{abc/\alpha\beta}$, and $T_{\alpha\beta/dq}$. In this scheme, DC offset voltage is measured by using the differential amplifier and an additional DC suppression loop is employed to suppress the DC injection. It is robust against the noise. The experimental results demonstrate the absolute value of dc injection current is below 5 mA in all three phases when the output power of the inverter changes from 15% to rated power. However, the main drawback of this scheme is that it cannot mitigate DC injection generated due to the unbalanced grid voltage and DC component in the grid voltage. Besides, the accuracy of the measured DC-offset voltage is limited by the differential amplifier and low-pass filter. The DC offset voltage is very small, which requires that the differential amplifiers have very high accuracy. Moreover, the cut-off frequency of the low-pass filter is expected to be very low to obtain high accuracy, but that will increase the cost.

Zhang, Xu, Ai, and Wu proposed a control strategy using an additional PI controller employed to control the reference current [34]. From Fig. 18, the difference between zero and the DC component I_{DC} input to the PI controller.

The basic idea of deadbeat control in power converter control is predicting the duty cycle of the next period according to the system status in the current period. In [35], Jia and Luo proposed a control strategy based on deadbeat control. As shown in (12), current compensation component $K_i \times I_\varepsilon$ is added to the current control. The injected DC component is suppressed in every period until the index I_ε is zero. The duty cycle in the next sampling point is derived by.

$$D(k+1) = \frac{\left\{\frac{L}{T_s}\left[i_{Lref}(k+1) - i_L(k)\right] + \overline{U_{ac}}(k+1) - K_i \times I_\varepsilon\right\}}{U_{dc}} \tag{12}$$

where $\overline{U_{ac}}(k+1)$ is the average value of grid voltage at the $k+1$ sampling period. T_s is the switching period of power switches. $i_L(k)$ and $i_{Lref}(k)$ are the inductance current and reference inductance current at k and $k+1$, respectively. U_{dc} is the input DC voltage, and $D(k+1)$ is the duty cycle of the PWM wave at the $k+1$ period. L is the inductance of the LC-type grid-connected converter.

In this algorithm, 20 points, which are symmetrical on the peak value, are used to calculate the DC component. I_ε is defined as

$$I_\varepsilon = i_L(i) + i_L(i+1) + \cdots + i_L(i+20) + i_L(N-i-20) + \cdots + i_L(N-i) \tag{13}$$

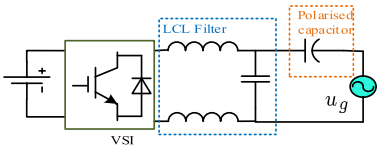

FIGURE 19. Basic theory of capacitor blocking method for DC component mitigation.

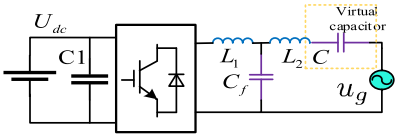

FIGURE 20. DC suppression with virtual capacitors.

If no DC component exists in the grid current, the sum of all sampled currents I_ε is zero. Otherwise, I_ε does not equal to zero and the larger I_ε is the larger DC component exists in the grid current. In the deadbeat current control loop, a proportional coefficient K_i is multiplied by I_ε as negative feedback compensation. From the experimental results, the absolute value of dc injection current is about 5 mA. It is worth to mention that K_i is closely related to the circuit structure, so it is necessary to select K_i properly according to the situation to achieve fast and stable DC suppression.

Compared with the above dc component suppression method, the dc current suppression converter is the simplest, the suppression method using voltage detection has the fast time response, and the method with dc suppression loop needs fast calculation and high-speed microprocessor.

C. CAPACITOR BLOCKING METHOD FOR DC COMPONENT MITIGATION

Considering the DC mitigation behaviour of capacitors, DC suppression scheme with physical blocking capacitors and virtual capacitors are presented in recent literatures.

1) PHYSICAL BLOCKING CAPACITORS

DC component blocking in this method can be realized by inserting the capacitors into grid current path of the circuit. In [19], Blewitt et al. proposed that a single electrolytic capacitor with large capacitance which is inserted into the circuit to block the DC component injecting into the grid. The power circuit topology is shown in Fig. 19, where the physical capacitors are inserted between the grid and the filter to block dc component.

Based on this idea, the blocking capacitors can be inserted at either inverter-side or grid-side inductance, for inverter-side capacitor, it can only suppress the dc component generated by the power converter, however, it cannot suppress the dc component generated by the dc-voltage or unbalanced grid. As a result, it is suggested to place the physical capacitors on the grid-current path.

Many advantages of single-layer aluminum electrolytic capacitors make them be an excellent choice for DC component blocking. More specifically, these capacitors are relatively cheap and smaller with large capacitance. Large capacitance will have low reactance at the fundamental frequency, which means the voltage-drop across the capacitor is small. However, this method has numerous disadvantages.

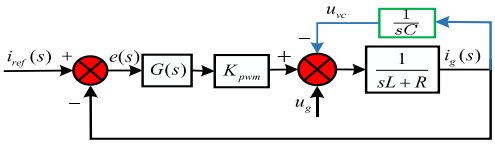

FIGURE 21. Block diagram of the virtual capacitor method.

- Realizing the gain across the capacitor at 50 Hz to be approximately 1, the capacitance should be designed to be relatively large. This may lead to increased cost and size for the power converters.
- To prevent the capacitor from disconnecting with the grid, auxiliary circuits are needed, which increases the complexity of the circuit and control strategy.
- Malfunction of the capacitors may disconnect the converter from the grid. This causes the breakdown of the whole system. Hence, nowadays, much attention has been paid on virtual capacitors.

2) VIRTUAL CAPACITORS

To replace physical capacitors, a dc suppression method based on virtual capacitors is proposed [36]–[38]. This method utilizes a closed-loop strategy to realize the equivalent function of a real capacitor. Fig. 20 shows a single-phase GCC with virtual dc component blocking capacitors.

Compared to the grid frequency, the switching frequency is high, the control loop block diagram can be determined according to the diagram of a single-phase GCC with DC blocking capacitor, which is shown in Fig. 21.

In [37], Wang et al. improved this method by adding an additional feedforward control to mitigate the burden of the current controller. In order to eliminate the influence of grid voltage, such as harmonics in grid voltage, the voltage feedforward control is used. The experiment shows the dc component is 0.016 Arms, which is about 0.38% of the rated current. Compared with physical capacitors, this method is easy to be realized. It requires no additional measurement circuit or other hardware for dc current detection. The DC suppression performance can be achieved by just modifying the software, which means that the method is simple and low-cost.

For the LCL-type grid-connected converter, the virtual capacitor method also can be used to suppress the DC component. In [39], Yang, Su and et al. proposed a control strategy based on the virtual capacitor method to suppress the DC component, in which an additional suppression control loop is employed to increase the output resistance of the DC component to suppress DC injection for grid-converters.

To extend this method in three-phase system, In [40], the Wang Wei and Bo Long, etc. extend the virtual capacitor concept into LCL-filter three-phase GCCs, where the

TABLE 5. Comparisons between different DC component suppression methods.

	Methods	Advantages	Disadvantages
DC current suppression converters	● Half-bridge converter [20, 29-31]. ● Improved single-phase three-level diode-clamped converter [31]. ● Other power circuit with capacitors in the loop.	● Relatively simple. ● No impact on the original system. ● No need for additional control. ● The capacitor voltages are not equal.	● High voltage stress for switching devices. ● Not suitable for large power output system.
DC compensation method	● Additional DC component suppression loop controller [32]. ● Additional current sampling circuit [34]. ● Improved compensation method based on deadbeat control [35]. ● DC voltage detection and compensation.	● Good suppression performance. ● No influences on the original control loop in the system. ● Good dc component suppression performance.	● Highly dependent on the measuring accuracy of the DC component in the grid current. ● Influences on the original system. ● The control algorithm is complex. ● High-speed calculation requirements for the microprocessor.
Capacitor blocking method	● Physical blocking capacitor [20]. ● Any other physical blocking capacitors in the grid-side inductance.	● Good suppression performance. ● Simple in implementation.	● Increased size and cost. ● Require additional protection circuit for converter. ● Hard to determine the optimal capacitance.
	● Virtual blocking capacitor [36-39].	● Good suppression performance. ● Relatively simple and flexible in the regulation of virtual capacitance. ● No need for DC component detection. ● Little impact on the original system.	● Hard to determine the optimal capacitance. ● Adding an additional resonant frequency point.
Intelligent control method	● Iteration PI control [6, 41] ● Neural Network Control [23].	● More robust for DC component suppression. ● Control parameter self-learning capability.	● Occupy large microprocessor on-chip resources. ● Complicated control algorithms. ● Need high-speed microprocessor for fast calculation.

blocking capacitors were inserted at the path of the grid-side current. This scheme is successfully suppressed the dc components and attenuated to 0.22%, 0.05% and 0.17% of the rated current for each phase. From the power circuit topology of the system, the transfer function of the open loop system is a fourth-order system, and there are two resonant points. Improper selection of the virtual capacitance will cause the system entering an unsteady state. As a result, it is needed to design a current controller which can ensure the stability of the system and meanwhile could realize fast-speed and high-resolution current tracking capability.

D. INTELLIGENT CONTROL METHOD

With the development of high-speed microprocessor (e.g. digital-signal-processor (DSP) and Field-Programmable-Gate-Array (FPGA)), the calculation capacity increases dramatically, which enables the intelligent control to be practical. Some literatures have discussed using iteration PI control in dc suppression, which has much better performance on decreasing the static error than traditional PI controller [41]. The iteration controller integrates the errors at the same sampling point in every period. Hence, it has better performance on static error suppression. However, its robustness and dynamic response cannot meet the requirements. However, they can be improved by using neural network (NN). In [23], the author proposed an intelligent control strategy

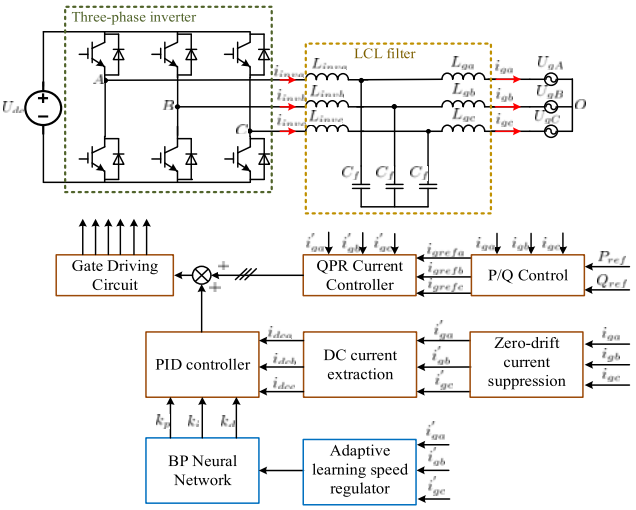

FIGURE 22. Block diagram of the DC component suppression scheme using BP -PID controller [23].

through utilizing adaptive-back-propagation (ABP) neural network PID controller in DC mitigation. Coefficients of the PID controller are on-line regulated by BP neural network output for DC component injection minimization.

Fig.22 shows a block diagram of the intelligent control scheme, where QPR current controller is used for accurate current tracking and the PID controller is used to suppress

the DC current. The ABP neural network is used to tune coefficients of the PID controller periodically. The experimental results show that the BP-PID control has a better performance than traditional PID control.

The disadvantages of the intelligent control in DC mitigation are that it requires large microprocessor RAM, ROM resources, and needs high-speed microprocessor for data storing and calculation. To show the advantage and disadvantage of different dc mitigation scheme, comparisons are presented in Table 5.

V. CONCLUSIONS

In this paper, a comprehensive review on DC component generation, detriments, detection and suppression method are demonstrated. For dc component detection, as shown in Table 4, it can be divided into two categories:

1) Hardware detection method. An auxiliary circuit is included for DC component detection, which contains four types, including methods based on transformers, two-stage single-order circuit, parallel-connected resonance circuit, and methods based on reactors. Due to the additional circuit, cost and complexity of the original system will increase. However, it does not have the time-delay in dc detection.
2) Software detection method. An algorithm such as SWDIM is implemented to realize dc detection. This method will not introduce additional cost, but it has the drawbacks of additional time-delay.

For dc suppression, to clearly show the typical features of those methods, comparisons between different dc suppression methods are summarized in Table 5.

1) DC suppression converters. This method suppresses dc component in the grid current through modifying the topology of GCCs including half-bridge converters and improved single-phase three-level diode-clamped converters. The improved topology can successfully suppress the DC component in the grid current and decrease the cost of TGCCs.
2) DC compensation methods. This method is highly dependent on high resolution dc detection existed in the grid current. Increasing the dc detection accuracy and decreasing its impacts on the system are the key points for this method.
3) Capacitor blocking method. Due to the disadvantages of physical capacitors, virtual capacitor method is more popular. Virtual capacitance selection is important for the overall system performance, which is a key point for this method.
4) Intelligent control. Currently, only a few literatures have been found in this area. In the author's perspective, the intelligent control for DC suppression should be paid more attention in the future.

ACKNOWLEDGMENT

The authors would like to thank all the reviewers for their advices and suggestions on improving this paper.

REFERENCES

[1] R. Sharma, "Removal of DC offset current from transformerless PV inverters connected to utility," in *Proc. 40th Int. Universities Power Eng. Conf.*, Jul. 2005, pp. 1230–1234.
[2] T. L. Ahfock and L. Bowtell, "DC offset elimination in a single-phase grid-connected photovoltaic system," in *Proc. 16th Australas. Universities Power Eng. Conf.*, 2006, pp. 1–9.
[3] A. Abdelhakim, P. Mattavelli, D. Yang, and F. Blaabjerg, "Coupled-inductor-based DC current measurement technique for transformerless grid-tied inverters," *IEEE Trans. Power Electron.*, vol. 33, no. 1, pp. 18–23, Jan. 2018.
[4] L. Bowtell and A. Ahfock, "Direct current offset controller for transformerless single-phase photovoltaic grid-connected inverters," *IET Renew. Power Generat.*, vol. 4, no. 5, pp. 428–437, Sep. 2010.
[5] A. Ahmed and R. Li, "Precise detection and elimination of grid injected DC from single phase inverters," *Int. J. Precis. Eng. Manuf.*, vol. 13, no. 8, pp. 1341–1347, Aug. 2012.
[6] C. Shu, "The cause and suppression strategy of DC component of three-phase PV grid connected inverter," *Telecom. Power Technol.*, vol. 34, no. 6, pp. 281–282, 2017.
[7] Q. N. Trinh, W. Peng, Y. Tang, and F. H. Choo, "Mitigation of DC and harmonic currents generated by voltage measurement errors and grid voltage distortions in transformerless grid-connected inverters," *IEEE Trans. Energy Convers.*, vol. 33, no. 2, pp. 801–813, Jun. 2017.
[8] G. Buticchi, E. Lorenzani, and G. Franceschini, "A DC offset current compensation strategy in transformerless grid-connected power converters," *IEEE Trans. Power Del.*, vol. 26, no. 4, pp. 2743–2751, Oct. 2011.
[9] S. N. Vukosavic and L. S. Perić, "High-precision active suppression of DC bias in AC grids by grid-connected power converters," *IEEE Trans. Ind. Electron.*, vol. 64, no. 1, pp. 857–865, Jan. 2017.
[10] S. B. Kjaer, J. K. Pederson, and F. Blaabjerg, "A review of single-phase grid-connected inverters for photovoltaic modules," *IEEE Trans. Ind. Appl.*, vol. 41, no. 5, pp. 1292–1306, Sep./Oct. 2005.
[11] W. Bower, F. Schalles, and T. Key, *Utility Compatibility of Nonisolated Residential Power Conditioners* Sandia National Labs., Albuquerque, NM, USA, 1987.
[12] H. Haeberlin, "Evolution of inverters for grid connected PV-systems from 1989 to 2000," in *Proc. 17th Eur. Photovoltaic Solar Energy Conf.*, 2001, pp. 1–2.
[13] M. Armstrong, D. J. Atkinson, C. M. Johnson, and T. D. Abeyasekera, "Auto-calibrating DC link current sensing technique for transformerless, grid connected, H-bridge inverter systems," *IEEE Trans. Power Electron.*, vol. 21, no. 5, pp. 1385–1393, Sep. 2006.
[14] F. Berba, D. Atkinson, and M. Armstrong, "A new approach of prevention of DC current component in transformerless grid-connected PV inverter application," in *Proc. IEEE 5th Int. Symp. Power Electron. Distrib. Gener. Syst. (PEDG)*, Jun. 2014, pp. 1–7.
[15] M. Calais, V. G. Agelidis, and M. S. Dymond, "A cascaded inverter for transformerless single-phase grid-connected photovoltaic systems," *Renew. Energy*, vol. 22, nos. 1–3, pp. 255–262, Jan. 2001.
[16] B. Wang, X. Guo, H. Gu, Q. Mei, and W. Wu, "Real-time DC injection measurement technique for transformerless PV systems," in *Proc. IEEE Int. Symp. Power Electron. Distrib. Gener. Syst.*, Jun. 2010, pp. 980–983.
[17] J. Jiang and X. Yuan, "Differential DC component suppression in three-phase non-isolated connected inverter," *Power Capacitor Reactive Power Compensation*, vol. 39, no. 1, pp. 132–137, 2018.
[18] T. Kerekes, R. Teodorescu, P. Rodríguez, G. Vázquez, and E. Aldabas, "A new high-efficiency single-phase transformerless PV inverter topology," *IEEE Trans. Ind. Electron.*, vol. 58, no. 1, pp. 184–191, Jan. 2011.
[19] W. M. Blewitt, D. J. Atkinson, J. Kelly, and R. A. Lakin, "Approach to low-cost prevention of DC injection in transformerless grid connected inverters," *IET Power Electron.*, vol. 3, no. 1, pp. 111–119, Jan. 2010.
[20] R. González, E. Gubía, J. López, and L. Marroyo, "Transformerless single-phase multilevel-based photovoltaic inverter," *IEEE Trans. Ind. Electron.*, vol. 55, no. 7, pp. 2694–2702, Jul. 2008.
[21] E. Gubía, P. Sanchis, A. Ursúa, J. López, and L. Marroyo, "Ground currents in single-phase transformerless photovoltaic systems," *Progr. Photovolt. Res.Applications*, vol. 15, no. 7, pp. 629–650, Nov. 2010.
[22] L. Cristaldi, A. Ferrero, M. Lazzaroni, and R. T. Ottoboni, "A linearization method for commercial Hall-effect current transducers," *IEEE Trans. Instrum. Meas.*, vol. 50, no. 5, pp. 1149–1153, Oct. 2001.

[23] B. Long, L. Huang, H. B. Sun, Y. Chen, F. Victor, and K. T. Chong, "An intelligent dc current minimization method for transformerless grid-connected photovoltaic inverters," *ISA Trans.*, vol. 88, pp. 268–279, May 2018.
[24] V. Salas, E. Olias, M. Alonso, F. Chenlo, and A. Barrado, "DC current injection into the network from PV grid inverters," in *Proc. IEEE World Conf. Photovoltaic Energy Conf.*, May 2006, pp. 2371–2374.
[25] W. Enders, C. Halter, and P. Wurm, "Investigation of typical problems of PV-inverters," in *Proc. Eur. Photovoltaic Solar Energy Conf.*, Oct. 2001, pp. 763–767.
[26] V. Salas, E. Olías, M. Alonso, and F. Chenlo, "Overview of the legislation of DC injection in the network for low voltage small grid-connected PV systems in Spain and other countries," *Renew. Sustain. Energy Rev.*, vol. 12, no. 2, pp. 575–583, Feb. 2008.
[27] F. Berba, D. Atkinson, and M. Armstrong, "A review of minimisation of output DC current component methods in single-phase grid-connected inverters PV applications," in *Proc. 2nd Int. Symp. Environ. Friendly Energies Appl.*, Jun. 2012, pp. 296–301.
[28] *Photovoltaic (PV) Systems—Characteristics of the Utility Interface*, document IEC61727, Europe, 2006.
[29] R. Gonzalez, J. López, P. Sanchis, and L. Marroyo, "Transformerless inverter for single-phase photovoltaic systems," *IEEE Trans. Power Electron.*, vol. 22, no. 2, pp. 693–697, Mar. 2007.
[30] T. F. Wu, H. S. Nien, H. M. Hsieh, and C. L. Shen, "PV power injection and active power filtering with amplitude-clamping and amplitude-scaling algorithms," *IEEE Trans. Ind. Appl.*, vol. 43, no. 3, pp. 731–741, May 2007.
[31] T. Shimizu, O. Hashimoto, and G. Kimura, "A novel high-performance utility-interactive photovoltaic inverter system," *IEEE Trans. Power Electron.*, vol. 18, no. 2, pp. 704–711, Mar. 2003.
[32] G. He, D. Xu, and M. Chen, "A novel control strategy of suppressing DC current injection to the grid for single-phase PV inverter," *IEEE Trans. Power Electron.*, vol. 30, no. 3, pp. 1266–1274, Mar. 2015.
[33] M. Chen, D. Xu, T. Zhang, K. Shi, G. He, and K. Rajashekara, "A novel DC current injection suppression method for three-phase grid-connected inverter without the isolation transformer," *IEEE Trans. Industrial Electron.*, vol. 65, no. 11, pp. 8656–8666, Nov. 2018.
[34] B. Zhang, F. Xu, Q. Ai, and L. Wu, "Dectecting and suppressing method for DC injection of grid-connected inverter under nonideal grid condition," *ACTA Energiae Solaris Sinica*, vol. 39, no. 12, pp. 3413–3420, 2018.
[35] D. Jia and L. Luo, "Causes and suppression of DC injection for single-phase photovoltaic inverter," *Modern Electron. Tech.*, vol. 6, p. 45, Jun. 2014.
[36] X. Guo, H. Gu, and G. San, "DC injection control for grid-connected inverters based on virtual capacitor concept," in *Proc. Int. Conf. Elect. Mach. Syst.*, Oct. 2008, pp. 2327–2330.
[37] W. Wang, P. Wang, T. Bei, and M. Cai, "DC injection control for grid-connected single-phase inverters based on virtual capacitor," *J. Power Electron.*, vol. 15, no. 5, pp. 1338–1347, Sep. 2015.
[38] B. Wang, X. Guo, Q. Mei, X. Sun, and W. Wu, "DC injection control for transformerless PV grid-connected inverters," *Proc. CSEE*, vol. 29, no. 36, pp. 23–28, Jun. 2009.
[39] L. Yang, "DC component suppression strategy for single-phase grid-connected inverter," *Electric Power Autom. Equip.*, vol. 35, no. 4, pp. 145–146, 2015.
[40] B. Long, "Design and implementation of a virtual capacitor based DC current suppression method for grid-connected inverters," *ISA Trans.*, 2019. doi: 10.1016/j.isatra.2019.02.019.
[41] P. Xu and L. Wu, "Suppression strategy of DC component based on fuzzy iteration PI," *J. Jiangnan Univ.*, vol. 14, no. 5, pp. 585–589, 2015.

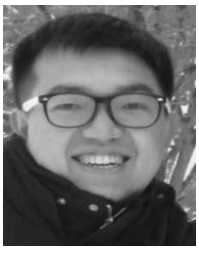

BO LONG received the B.S. degree in electrical engineering from Xi'an Petroleum University, Xi'an, China, in 2001, and the Ph.D. degree in electrical engineering from Xian Jiaotong University, Shanxi, China, in 2008. He joined the Department of Power Electronics, School of Mechatronics Engineering, University of Electronic Science and Technology of China (UESTC), in 2008, and was promoted to Associate Professor, in 2014. From 2017 to 2018, he was a Visiting Scholar (Guest Post-Doctoral Researcher) in the area of renewable energy and microgrids with the Department of Electrical Engineering, Tsinghua University, Beijing, China. His research interests include ac/dc microgrids, grid-connected converters for renewable energy systems and DGs, model predictive control, power quality, multilevel converters, ac motor control, and resonance suppression technique for smart grid applications. He has authored over 20 SCIE-indexed journal papers and one book chapter in the areas of power electronics, motor control, battery management system, and smart grid. He has seven issued and ten pending patents. He is currently a Supervisor for 11 master students, 2 of which have been nominated as provincial outstanding graduate student of UESTC. He is also an active Reviewer of the IEEE TRANSACTIONS ON POWER ELECTRONICS, *ISA Transactions*, *Applied Energy*, *Energy*, the IEEE TRANSACTIONS ON SMART GRID, the IEEE TRANSACTIONS ON INDUSTRIAL ELECTRONICS, the IEEE TRANSACTIONS ON SUSTAINABLE ENERGY, and the IEEE TRANSACTIONS ON ENERGY CONVERSION.

MUHENG ZHANG received the B.Eng. degree in electronic information engineering from the University of Electronic Science and Technology of China, in 2019. He is currently pursuing the M.S. degree in electronic and electrical engineering with the University of California at Irvine. His current research interests include the dc component suppression for inverter, motor control, micro-grid systems, and renewable energy sources.

YONG LIAO received the B.S. degree in mechanical engineering from Southeast University, Nanjing, China, in 2017. He is currently pursuing the M.S. degree in mechanical engineering with the University of Electronic Science and Technology of China, Chengdu, China. His current research interests include the optimization of ac microgrids, power distribution, and current circulation suppression between the inverters.

LIJUN HUANG received the B.S. degree in electrical engineering and automation from the University of Electronic Science and Technology of China, Chengdu, China, in 2016, and the M.S. degree from the School of Mechanical and Electrical Engineering, University of Electronic Science and Technology of China, in 2019. She is currently with Guangzhou Haige Communication Group Incorporated Company, Guangzhou, China. Her research interests include optimization of ac microgrids, dc component suppression, motor drive systems, grid-integration of renewable energy resources, and signal processing field.

KIL TO CHONG received the Ph.D. degree in mechanical engineering from Texas A&M University, in 1995. He is currently a Professor and the Department Head of the School of Electronics and Information Engineering and a member and the Head of the Advanced Electronics and Information Research Center, Chonbuk National University, Jeonju, South Korea. His research interests include motor fault detection and control, network system control, sensor network systems, time-delay systems, and neural networks.